

Widespread expression of erythropoietin receptor in brain and its induction by injury

Christoph Ott MSc¹, Henrik Martens PhD², Imam Hassouna PhD^{1§}, Bárbara Oliveira MSc¹,
Christian Erck PhD², Maria-Patapia Zafeiriou PhD³, Ulla-Kaisa Peteri BSc¹, Dörte Hesse⁴,
Simone Gerhart¹, Bekir Altas MSc⁵, Tekla Kolbow², Herbert Stadler PhD², Hiroshi Kawabe MD⁵,
Wolfram-Hubertus Zimmermann MD³, Klaus-Armin Nave PhD^{6,7},
Walter Schulz-Schaeffer MD⁸, Olaf Jahn PhD^{4,7}, and Hannelore Ehrenreich MD DVM^{1,7*}

¹Clinical Neuroscience, Max Planck Institute of Experimental Medicine,

²Synaptic Systems GmbH,

³Institute of Pharmacology, University Medical Center,

⁴Proteomics Group, Max Planck Institute of Experimental Medicine,

⁵Molecular Neurobiology, Max Planck Institute of Experimental Medicine,

⁶Neurogenetics, Max Planck Institute of Experimental Medicine,

⁷DFG Center for Nanoscale Microscopy and Molecular Physiology of the Brain (CNMPB),

⁸Department of Neuropathology, University Medical Center,

Göttingen, Germany

[§]IH is co-affiliated to the Physiology Unit, Zoology Department, Faculty of Science,

Menoufia University, Egypt

Running head: EPOR in brain

Key words:

EPOR antibody, mass spectrometry, central nervous system, stab wound, epilepsy

***Correspondence:**

Prof. Hannelore Ehrenreich, MD, DVM

Clinical Neuroscience

Max Planck Institute of Experimental Medicine

Göttingen, Germany

Phone +49-551-3899615

Fax +49-551-3899670

Email: ehrenreich@em.mpg.de

ABSTRACT

Erythropoietin (EPO) exerts potent neuroprotective, neuroregenerative and procognitive functions. However, unequivocal demonstration of erythropoietin receptor (EPOR) expression in brain cells has remained difficult since previously available anti-EPOR antibodies (EPOR-AB) were unspecific. We report here a new, highly specific, polyclonal rabbit EPOR-AB directed against different epitopes in the cytoplasmic tail of human and murine EPOR and its characterization by mass spectrometric analysis of immunoprecipitated endogenous EPOR, Western blotting, immunostaining, and flow cytometry. Among others, we applied genetic strategies including overexpression, Lentivirus-mediated conditional knockout of *EpoR*, and tagged proteins, both on cultured cells and tissue sections, as well as intracortical implantation of *EPOR*-transduced cells to verify specificity. We show examples of EPOR expression in neurons, oligodendroglia, astrocytes, and microglia. Employing this new EPOR-AB with double-labelling strategies, we demonstrate membrane expression of EPOR as well as its localization in intracellular compartments such as the Golgi apparatus. Moreover, we show injury-induced expression of EPOR: In mice, a stereotactically applied stab wound to the motor cortex leads to distinct EpoR expression by reactive GFAP-expressing cells in the lesion vicinity. In a patient suffering from epilepsy, neurons and oligodendrocytes of the hippocampus strongly express EPOR. To conclude, this new analytical tool will allow neuroscientists to pinpoint EPOR expression in cells of the nervous system and to better understand its role in healthy conditions, including brain development, as well as under pathological circumstances, such as upregulation upon distress and injury.

UNCORRECTED PROOF

INTRODUCTION

The growth factor erythropoietin (EPO) was named based on its first discovered effects on cells of the hematopoietic system. For >20 years it has been shown to act on other tissues, including the brain, e.g. (1-5). Its remarkable neuroprotective, neuroregenerative and procognitive effects make EPO an attractive candidate for treating human brain disease, e.g. (6-7), and an important target of neuroscience research. In 1989, the EPO receptor (*EpoR*) has first been cloned in mouse (8), soon followed by cloning and characterization of the human *EPOR* gene (9-10). A single EPO molecule binds to 2 specific cytokine type1 transmembrane receptor molecules, each with a calculated molecular mass of 59kDa, that together form the classical homodimeric EPOR (2, 11). Binding of EPO to its receptor induces a conformational change, initiating EPOR-associated JAK2 transphosphorylation and multiple, cell-type specific, downstream signal transduction cascades. These cascades include signal transducers and activators of transcription (STATs), phosphatidylinositol-3 kinase (PI3K)/AKT, RAS/extracellular signal-regulated kinase (ERK1/2), nuclear factor kappa B (NF-kappa B). Activation of these signaling cascades leads to further activation of anti-apoptotic factors and pathways, stimulation of cell differentiation, including induction of cellular shape-change and growth, or modulation of plasticity, in a cell-type and stimulation-dependent manner (5, 12-13).

Antibodies against EPOR (EPOR-AB) have been widely used to characterize EPOR expression and localization, but cell surface EPOR expression is low, even in stimulated states, and most importantly, all commercially available EPOR-AB have been hampered by non-specific cross-reactivities, questioning the exclusively hereon based literature. This in turn raised discussions within the scientific community, questioning the expression of EPOR in extra-hematopoietic tissues (14-16). These discussions were likely nurtured by conflicts of interest, trying to 'restrict' the effects of EPO, a commercially for the anemia market highly attractive compound, to hematopoiesis. Nevertheless, they made it very obvious that the existing EPOR-AB were essentially unreliable, and that the production and thorough characterization of new and more specific EPOR-AB had to be seen as a major challenge for the future (14, 17-18).

Independent of work based on EPOR-AB, genetically altered mice helped to demonstrate that EPOR signalling is necessary for normal brain development (19) and that it has a distinct function in neurogenesis (20). In addition, EPO and EPOR mRNA are expressed in brain tissue (21), and specific binding sites for EPO in brain have been demonstrated in mouse and human by means of radiolabelled EPO (22-23). In cell culture, mRNA expression combined with functional assays, e.g. altered phosphorylation of second messenger pathways induced by EPO in microglia, served to prove specific EPOR expression in the absence of reliable EPOR-AB (24).

The fact that cellular EPOR protein expression has been difficult to assess, strongly limited the in-depth investigation of the EPO/EPOR system. Particularly in the human brain, the study of its (patho-) physiological role has been highly constrained since additional means of verification as used in experimental animals and cell cultures are naturally excluded. Recognizing this critical issue in EPO/EPOR research, we aimed at generating reliable EPOR-AB. We present here the comprehensive characterization of a novel, highly specific EPOR-AB, using an array of state-of-the-art technologies. This new AB tool may help overcome the described obstacles and lead to revisiting some of the reported data.

MATERIALS AND METHODS

Generation of EPOR-AB

Polyclonal AB

Two rabbits were immunized with a purified recombinant protein corresponding to amino acids (AA) 273-508 (intracellular C-terminus) of the unprocessed human EPOR. The coding sequence was generated by gene synthesis (Geneart, Regensburg, Germany) and ligated via EcoRI and HindIII into the bacterial expression vector pASK-IBA37+ (IBA-Lifescience, Göttingen, Germany). The recombinant His-Tag fusion protein was expressed and purified by Ni-NTA affinity chromatography according to the manufacturer's manual. Crude antiserum SA7378 was affinity purified with the immunogen coupled to CNBr Sepharose (GE-

Healthcare, Freiburg, Germany). The AB is referred to as ctEPOR-AB in this manuscript.

Monoclonal AB

AB producing hybridomas were generated by Synaptic Systems (Göttingen; see also <http://www.sysy.com/mabservice.html>) as follows: Three 8–10 weeks old BALB/c female mice were subcutaneously immunized with a synthetic peptide corresponding to AA 25-39 (extracellular N-terminus) of unprocessed human EPOR precursor coupled to KLH via a C-terminal cysteine over a period of 75 days. Cells from the knee lymph nodes were fused with the mouse myeloma cell line P3X63Ag8.653 (ATCC CRL-1580). Resulting hybridomas were screened by direct ELISA against the immunogen and immunofluorescence on 3T3 NIH fibroblasts overexpressing full-length human EPOR. Clone 45A3, used in this study, was re-cloned two times by limiting dilution and the immunoglobulin subclass was determined (IgG2b). The AB is referred to as ntEPOR-AB in this manuscript.

Cell culture

Cell lines

The following human cell lines were used: **[1] The EPO-dependent megakaryoblastic leukaemia UT-7 cell line** (kind gift from Drorit Neumann, Tel Aviv University, Israel). This cell line was cultured in IMDM with 1% GlutaMAX supplement (Invitrogen, Darmstadt, Germany), 10% FBS, 100U/mL penicillin and 100µg/mL streptomycin (all Life Technologies GmbH, Darmstadt, Germany) and 2IU/mL EPO (NeoRecormon, Roche, Welwyn Garden City); **[2] The erythroleukaemia cell line OCIM-1** (DSMZ GmbH, Braunschweig, Germany) was cultured in IMDM with 1% GlutaMAX supplement, 10% FBS and 100U/mL penicillin and 100µg/mL streptomycin (all Life Technologies GmbH); **[3] The mouse microglia cell line EOC-20** (ATTC LGC Standards, Wesel, Germany) was cultured in DMEM with 1mM sodium pyruvate, 0.15% sodium bicarbonate, 10% FBS, 100U/mL penicillin, 100µg/mL streptomycin (all Life Technologies GmbH) and 0.01 µg/mL murine M-CSF (PAN-Biotech, Aidenbach, Germany); **[4] HEK293 FT cells** (Sigma-Aldrich, Taufkirchen, Germany) were cultured in DMEM with 5 % FBS and 100U/mL penicillin and 100µg/mL streptomycin (all Life Technologies GmbH).

Human IPS cells

Human material was used in accordance with ethical guidelines and the Helsinki Declaration. Subjects gave informed consent regarding generation and use of IPS cells or scientific investigation of brain samples. Human fibroblasts were reprogrammed using a non-integrative RNA-based virus to induce the expression of 4 reprogramming factors: OCT4, SOX2, KLF4 and c-MYC (CytoTune®-iPS 2.0 Sendai Reprogramming Kit, Life Technologies GmbH). After transduction, IPS cells (clones isAu1-3; isAu3-2) were adapted to a feeder-free culture system (Matrigel® matrix, Corning, Wiesbaden, Germany) and cultured in TeSR™-E8™ medium (Stem Cell Technologies™, Cologne, Germany).

Primary mouse cell culture

The preparation and culture conditions of primary mouse oligodendrocytes and microglia are described in detail elsewhere (24-25). In brief, oligodendrocytes were prepared from the forebrains of newborn P1-2 NMRI mice. After differentiation, oligodendrocyte precursors were shaken off from a bottom layer of astrocytes and seeded in Super-Sato medium (DMEM with high glucose supplemented with B-27 supplement, 2mM GlutaMAX, 1mM sodium pyruvate, 1% horse serum (HS), 50U/mL penicillin and 50µg/mL streptomycin, all from Life Technologies GmbH) and 0.5mM triiodothyronine, and 0.52mM L-thyroxine both Merck, Darmstadt, Germany). For primary microglia, newborn C57BL6 mice (P0-P1) were used. The cell suspension derived from their forebrains was seeded in high glucose DMEM medium with 10% HS, 1% GlutaMAX supplement, 50U/mL penicillin and 50µg/ml streptomycin (all from Life Technologies GmbH). Half of the microglia-conditioned medium was exchanged by fresh medium 3-4 days later, and at day 7, the medium was partially replaced by L929-conditioned medium. Primary microglia were detached by shaking of flasks and seeded in serum-free microglial growth medium (high glucose DMEM with 1mM sodium pyruvate, 1.5g/L sodium bicarbonate, 100U/mL penicillin and 100µg/mL streptomycin, all from Life Technologies GmbH).

Lentiviral transduction of primary cells

EpoR conditional mouse mutants with floxed exons 3-6 were generated on the C57Bl/6 background by standard procedures using mutant ES cells

(EPD0316_5_A03) from the International Mouse Phenotyping Consortium. Details will be published elsewhere and are available upon request. Primary mouse astrocytes prepared from P0-2 forebrains of *EpoR-fl/fl* mice were used. The preparation and culture conditions of these cells are described in detail elsewhere (26). The cells were infected with lentiviruses at day1 *in vitro*. The viral constructs contained either a cassette for GFP only (control) or a cassette for GFP and Cre-recombinase. Protein was extracted on day10 *in vitro*.

EOC-20 cell transduction

For viral transduction 100,000 EOC-20 cells were seeded in 12-well plates overnight. The next day, the medium was partially exchanged by DMEM (Life Technologies GmbH) containing viral supernatant and 8µg/mL polybrene (Sigma-Aldrich). The ecotropic virus particles used were derived from a pMOWS vector encoding N-terminally HA-tagged full-length human *EPOR* and puromycin resistant cassettes (kind gift from Ursula Klingmüller, DKFZ Heidelberg, Germany) (27). Next, the 12-well plates were centrifuged for 3h at 1640rpm at room temperature (RT). The medium was exchanged again to DMEM with 1mM sodium pyruvate, 0.15% sodium bicarbonate, 10% FBS, 100U/mL penicillin, 100µg/mL streptomycin (all Life Technologies GmbH) and 0.01 µg/mL murine M-CSF (PAN-Biotech). The medium was supplemented 1 day later with 6µg/mL puromycin (Sigma-Aldrich) for selection of successfully transduced EOC-20 cells. After successful transduction, cells were constantly cultured in the presence of 6µg/mL puromycin.

HEK293 FT cell transfection

HEK293 FT cells were transfected with Lipofectamine®2000 reagent (Life Technologies GmbH) according to the manufacturer's instructions. The pEuExpress-hEPOR vector (Synaptic Systems, Göttingen, Germany) was used to transfect the cells with full-length human *EPOR* (~60 kDa), full-length murine *EpoR* (~60 kDa), an N-terminally HA-tagged and C-terminally truncated human *EPOR* (lacks the intracellular domain, ~40 kDa) and an anchored human *EPOR* (lacks the N-terminus and the C-terminus, ~12 kDa).

STAT5 phosphorylation assay

This assay is described in detail elsewhere (17). In brief, UT-7 or OCIM-1 cells were serum- and EPO-deprived overnight (1% FBS in IMDM, both Life Technologies GmbH). On the next day, they were incubated with different concentrations of recombinant human EPO (rhEPO, NeoRecormon, Roche) or control solution for 15min, followed by protein extraction for Western blotting. Immunodetection was done with anti-phosphorylated STAT5 (1:500, Cell Signaling, Danvers, MA, USA) and GAPDH (1:5000, Enzo Life Sciences, Farmingdale, NY, USA); 20µg of protein was loaded for SDS-PAGE.

MAPK phosphorylation assay

Transduced EOC-20 cells were kept in serum free DMEM (Life Technologies GmbH) overnight. Then, cells were incubated with different concentrations of rhEPO (NeoRecormon, Roche) or the respective control solution for 10 min, followed by protein extraction for Western blotting. Immunodetection was done with anti-phosphorylated MAPK (1:1000), anti-MAPK (1:5000) and anti-alpha-tubulin (1:5000, all from Sigma-Aldrich); 15µg of protein was loaded for SDS-PAGE.

Animal experiments

All experiments were approved by and conducted in accordance with the regulations of the local Animal Care and Use Committee (Niedersächsisches Landesamt für Verbraucherschutz und Lebensmittelsicherheit – LAVES).

Stereotactic cell implantation

Male C57BL/6N mice, 8 weeks old, were used. Animals were injected intraperitoneally (i.p.) with carprofen (5mg/kg Rimadyl®, Pfizer, Berlin, Germany) 2h before surgery. Under anaesthesia (0.276mg/g Tribromoethanol, Sigma-Aldrich, St. Luis, Minnesota, USA), mice were positioned in a stereotactic frame and a small, midline scalp incision was made. A hole was drilled over the left cranial hemisphere at a position 1.5mm anterior and 1.0mm lateral to the bregma. Using a sterile 10mL Hamilton syringe with a 26-gauge needle, 15,000 transduced EOC-20 cells (description see above) or medium only (DMEM without phenol-red, Life Technologies GmbH) were slowly (over 2min) implanted 2mm deep into the left M2

motor cortex. After implantation, the needle was left in place for 2min, then slowly withdrawn from the brain and the skin incision closed with sterile suture. Directly after the skin incision was closed, the animals received carprofen i.p. for pain treatment which was repeated every 6-8h (5mg/kg Rimadyl®, Pfizer). At 24h after surgery, animals were anesthetized i.p. (0.276mg/g Tribromoethanol; Sigma-Aldrich) and perfused transcardially with 0.9% saline followed by 4% formaldehyde in PBS.

Labelling of oligodendrocyte precursor cells in vivo

For induction of CreERT2-activity in NG2-Cre-ERT2:R26R-td-tomato-mEGFP mice (28-29), 100mg/kg tamoxifen (dissolved in corn oil; Sigma-Aldrich, Taufkirchen, Germany) was injected i.p. at postnatal days 26 and 27. At 72h later, animals were anesthetized i.p. (0.276mg/g Tribromoethanol, Sigma-Aldrich) and perfused transcardially with 0.9% saline followed by 4% formaldehyde in PBS.

Detection of EPOR

Immunoprecipitation

UT-7 protein lysates were obtained using an immunoprecipitation (IP) buffer (150mM NaCl, 20mM Tris, 1mM EDTA, 10% glycerol, pH=7.4) containing 1% Triton X-100. Before IP, lysates were diluted 1:1 with IP buffer to obtain 0.5% Triton X-100. For the EPOR IP, protein-G sepharose beads were covalently linked to ctEPOR-AB (Synaptic Systems) with 40mmol/L dimethyl-pimelimidate (Sigma-Aldrich). Bead slurry (200µL; Thermo Scientific, Waltham, MA, USA) was cross-linked with 400µg ctEPOR-AB or 400µg of the IgG fraction from the same rabbit before immunization. For EPOR IP from UT-7 protein lysates, 9µg of ctEPOR-AB coupled to protein-G sepharose per 1mg protein lysate were incubated for 2h at 4°C. Afterwards, beads were centrifuged and washed. For immunoblot analysis, EPOR was eluted from the beads by repeated boiling in Laemmli buffer at 95°C. For mass spectrometric protein identification, EPOR was eluted as before but with a non-reducing SDS-buffer (without β-mercaptoethanol) to prevent masking of the EPOR by excess AB heavy chains in the subsequent gel electrophoresis. To increase the efficiency of EPOR capture from UT-7 protein lysates, 2 consecutive IP with fresh beads were performed in a way that the flow-through of the first IP was used as input for the second. Eluted proteins were precipitated by methanol/chloroform treatment (30). Pellets were

solubilized in reducing sample buffer and pooled prior to electrophoresis. As starting material for mass spectrometry 4mg protein lysate from UT-7 cells was used.

SDS-PAGE and Western blots

SDS-PAGE was performed with self-made 10% SDS-polyacrylamide gels. As protein ladder we used PageRuler™ Plus pre-stained and SeeBlue Plus2 pre-stained in this gel system (both Life Technologies GmbH). For all Western blotting, the following protein amounts were loaded: [1] 15 µg for lysates derived from cell lines; [2] 20 µg for lysates derived from primary cultures; [3] 50 µg for lysates derived from tissue. Afterwards, proteins were transferred to a nitrocellulose membrane and blocked with 4% milk powder and 4% HS in Tris buffered saline with 0.05% Tween 20. Membranes were incubated with ctEPOR-AB (1:2000, Synaptic Systems) at 4°C overnight. For all EPOR immunoblots, membranes were washed, blocked again and incubated with donkey anti-rabbit IRDye 800 AB (1:10000, Rockland, Limerick, PA, USA) for 1h at RT. Primary mouse AB were detected with donkey anti-mouse IRDye 800 AB (1:10000, Rockland) for 1h at RT. After washing, the membranes were scanned with Odyssey imager (LI-COR Biosciences, Lincoln, NE, USA) and analyzed with the Image Studio software. Gel electrophoresis for mass spectrometric protein identification were performed in parallel on precast NuPAGE 4-12% Bis-Tris gradient gels using a 3-(N-morpholino)propanesulfonic acid (MOPS) buffer system according to the manufacturer (Invitrogen). As protein ladder we used SeeBlue Plus2 pre-stained in this gel system (Life Technologies GmbH). Proteins were either visualized by colloidal Coomassie staining (gel 1) or transferred on PVDF membranes and immunodetected as described above (gel 2).

Protein identification

Gel regions of interest were identified by overlaying images from colloidal Coomassie staining and immunodetection in the Delta 2D image analysis software (Decodon, Greifswald, Germany). Gel bands were excised manually and subjected to automated in-gel digestion with trypsin as described previously (31). Tryptic peptides were dried down in a vacuum centrifuge, re-dissolved 0.1 % trifluoro- acetic acid and spiked with 2.5fmol/µL of yeast enolase1 tryptic digest standard (Waters Corporation, Milford, MA, USA) for quantification purposes (32). Nanoscale reversed-phase UPLC

separation of tryptic peptides was performed with a nanoAcquity UPLC system equipped with a Symmetry C18 5 μ m, 180 μ m \times 20mm trap column and a BEH C18 1.7 μ m, 75 μ m \times 100mm analytical column (Waters Corporation). Peptides were separated over 60min at a flow rate of 300nL/min with a linear gradient of 1-45 % mobile phase B (acetonitrile containing 0.1 % formic acid) while mobile phase A was water containing 0.1 % formic acid. Mass spectrometric analysis of tryptic peptides was performed using a Synapt G2-S quadrupole time-of-flight mass spectrometer equipped with ion mobility option (Waters Corporation). Positive ions in the mass range m/z 50 to 2000 were acquired with a typical resolution of at least 20,000 FWHM (full width at half maximum) and data were lock mass corrected post-acquisition. With the aim of increasing the sequence coverage of the identified proteins, analyses were performed in the ion mobility-enhanced data-independent acquisition mode (33-34) with drift time-specific collision energies (35). For protein identification, continuum LC-MS data were processed and searched using Waters ProteinLynx Global Server version 3.0.2 (36). A custom database was compiled by adding the sequence information for yeast enolase 1 and porcine trypsin to the UniProtKB/Swiss-Prot human proteome (UniProtKB release 2015_06, 20,206 entries) and by appending the reversed sequence of each entry to enable the determination of false discovery rate (FDR). Precursor and fragment ion mass tolerances were automatically determined by PLGS 3.0.2 and were typically below 5ppm for precursor ions and below 10ppm (root mean square) for fragment ions. Carbamidomethylation of cysteine was specified as fixed and oxidation of methionine as variable modification. One missed trypsin cleavage was allowed. The FDR for protein identification was set to 1% threshold.

Flow cytometry

UT-7 cells were fixed with 4% Histofix solution (Carl Roth, Karlsruhe, Germany). For EPOR staining, cells were blocked, permeabilized with 5% normal horse serum (NHS) and 0.5% Triton X-100, and incubated with ctEPOR-AB (1:500, Synaptic Systems) and Hoechst (5 μ g/mL Invitrogen) or for control only Hoechst for 30min on ice. After washing, cell suspensions were incubated with Alexa488 donkey anti-rabbit (1:250, Life Technologies GmbH) for 30min on ice, followed by FACS analysis (FACSAria III, BD Biosciences, Heidelberg, Germany).

Immunocytochemistry

Cells were fixed with 4% formaldehyde in PBS for 20min, permeabilized and blocked in 0.2% Triton X-100 with 10% NHS in PBS for 20min. After washing with 1% NHS in PBS, cells were incubated overnight at 4°C with the primary AB in 0.2% Triton X-100 with 1% NHS in PBS. The following primary AB were used: Rabbit ctEPOR-AB (1:1000, Synaptic Systems), mouse ntEPOR-AB (1:1000, Synaptic Systems), mouse anti-HA (1:500, Covance Inc., Princeton, USA), mouse anti-GM130 (1:100, BD Biosciences, Heidelberg, Germany), rat anti-NG2 (1:250, kind gift from Dr Trotter, University of Mainz, Germany), goat anti-human Oct-3/4 (1:40, R&D Systems, Minneapolis, MN, USA). After washing, cells were incubated with the following secondary AB in 0.2% Triton X-100 with 1% NHS in PBS for 1h at RT: Donkey anti-rabbit Alexa488 and anti-goat Alexa488, donkey anti-mouse Alexa568, donkey anti-rabbit Alexa594 (all 1:500, Life Technologies GmbH) and goat anti-rat Alexa488 (1:250, Jackson ImmunoResearch, West Grove, PA, USA). Primary microglia were counterstained with tomato lectin Alexa488 (1:250, Vector Laboratories, Burlingame, CA, USA). Cell nuclei were visualized with DAPI dissolved in H₂O (0.01µg/mL, Sigma-Aldrich). Afterwards, the coverslips were dried and mounted with Aqua-Poly/Mount (Polysciences, Warrington, PA, USA). All stainings were scanned by confocal microscopy (TCS SP5-II, Leica, Wetzlar, Germany). Illustration was done using Imaris 7.5.1 (www.bitplane.com).

Immunohistochemistry on frozen mouse sections

C57BL6/N mice, 5 weeks old, were anesthetized by i.p. injection (0.276mg/g Tribromoethanol, Sigma-Aldrich) and perfused transcardially with 0.9% saline followed by 4% formaldehyde in PBS. Brains were removed, post-fixed overnight at 4°C with 4% formaldehyde in PBS and placed in 30% sucrose in PBS for cryoprotection and stored at -20°C. Whole mouse brains were cut into 30µm thick coronal sections on a cryostat (Leica). Frozen sections were permeabilized and blocked with 0.5% Triton X-100 and 5% NHS in PBS for 1h at RT. Then, sections were incubated with the following primary AB in 3% NHS, 0.5% Triton X-100 in PBS for 48h at 4°C: Rabbit ctEPOR-AB (1:200), chicken anti-NeuN (266 006; 1:500), guinea pig anti-GFAP (173 004; 1:500, all Synaptic Systems) and mouse anti-APC (clone CC-1, 1:100, Merck). After washing in PBS, sections were incubated with the

following secondary AB in 3% NHS, 0.5% Triton X-100 in PBS for 1.5h at RT: Donkey anti-rabbit Alexa594, donkey anti-mouse Alexa488 (both 1:500; Life Technologies GmbH), donkey anti-chicken (1:250), goat anti-guinea pig (1:300, both Jackson ImmunoResearch). Cell nuclei were visualized with DAPI dissolved in H₂O (0.01µg/mL, Sigma-Aldrich). After washing in PBS sections were mounted on Super Frost microscopic slides, dried and covered with Aqua-Poly/Mount (Polysciences). All stainings were scanned by confocal microscopy (TCS SP5-II, Leica). Illustration was done using Imaris 7.5.1 (www.bitplane.com).

Immunohistochemistry on paraffin embedded human brain sections

Brain slices of 1-3µm thickness from formalin-fixed and paraffin-embedded tissue blocks were deparaffinized. Endogenous peroxidases were blocked with 3% H₂O₂ in PBS for 20min followed by epitope blocking with 0.02% casein in PBS for 15min. Immunoreaction was performed by incubation with ctEPOR-AB (1:500, Synaptic Systems) over night at RT, followed by addition of the secondary biotinylated donkey anti-rabbit AB (1:500; Amersham Biosciences Freiburg, Germany) and an extravidin-peroxidase enzyme complex (1:1000; Sigma-Aldrich), each for 1h at RT. The AB reaction was visualized with the chromogen AEC: 4mL 4% 3-amino-9-ethylcarbazole (Sigma-Aldrich) in N,N-dimethylformamide (Merck) were dissolved in 56mL 0.1M sodium-acetate buffer adjusted to pH5.2 with acetic acid and 1% H₂O₂. The brain slices were counterstained with hemalum. Coverslips were mounted with Aquatex (Merck).

RESULTS

Generation of EPOR-AB

The aim of this work was to generate specific and sensitive EPOR-AB and to investigate EPOR expression in the central nervous system (CNS). Therefore, polyclonal rabbit EPOR-AB and monoclonal mouse EPOR-AB were produced and tested. After extensive characterization of a whole panel of AB (data not shown), 2 highly promising candidates were selected and validated for several research

purposes: (I) The polyclonal rabbit EPOR-AB SA7378, directed against the C-terminus (here always referred to as ctEPOR-AB) and (II) the monoclonal mouse EPOR-AB 45A3, directed against the N-terminus (here referred to as ntEPOR-AB). The present study is mainly built on ctEPOR-AB because of its high specificity and broad spectrum of applications in human and mouse.

Functional EPOR validation in the test systems

As prerequisite of testing EPOR-AB in the cell lines used here, we functionally validated their EPOR expression. In the EPO-dependent megakaryoblastic leukaemia cell line UT-7, incubation with different concentrations of rhEPO led to STAT-5 phosphorylation (Fig.1A). Also, in the erythroleukaemia cell line OCIM-1, incubation with rhEPO induced STAT-5 phosphorylation (Fig.1B). UT-7 cells only proliferated and survived in the presence of rhEPO in the medium (Fig.1C-D). In the mouse microglia cell line EOC-20, stably transduced with N-terminally HA-tagged human *EPOR*, rhEPO administration activated MAPK phosphorylation in a concentration-dependent manner (Fig.1E). We also confirmed *EPOR* mRNA expression in all of these cell lines by qPCR (normalized to GAPDH as housekeeping gene – data not shown).

Detection of EPOR/EpoR by Western blotting

To confirm reliable detection of EPOR by Western blotting, we transfected HEK293 FT cells with different *EPOR* expression vectors. The polyclonal rabbit ctEPOR-AB detected full-length human EPOR and its degradation product specifically while the C-terminally truncated mutant of EPOR was not detected by this AB (Figs.1F-G). Immunoblots of lysates from transduced EOC-20 cells (N-terminally HA-tagged human EPOR) and respective controls showed specific detection of full-length human EPOR by ctEPOR-AB (Fig.1H). This was validated with an HA immunoblot of the same lysates (Fig.1I). In protein lysates from UT-7 and OCIM-1 cells, ctEPOR-AB detected bands of the same molecular weight (Fig.1J). As shown in Fig.1F and J, in UT-7 cells and HEK293 FT cells (only when transfected with the full length human EPOR) a specific degradation product was additionally detected at ~40kDa by the ctEPOR-AB. This degradation product of EPOR has been described earlier (11). Fixed UT-7 cells were successfully used for flow cytometric analysis after staining

with ctEPOR-AB (Fig.1K). EPOR was further recognized by ctEPOR-AB in human placenta and fetal brain extracts (Fig.1L). In addition to human EPOR, ctEPOR-AB detected murine EpoR in transfected HEK293 FT cells, mouse fetal liver and lysates from cultured primary mouse oligodendrocytes (Fig.1M). To validate the specificity of murine EpoR detection, *EpoR* was knocked out in primary astrocytes derived from *EpoR-fl/fl* mice. In fact, ctEPOR-AB recognized a doublet of bands (EPOR with or without N-glycosylation, resulting in a difference of ~3kDa) with a molecular weight of around 65kDa (Fig.1N, control transduction). Shown is a clear reduction upon expression of Cre-recombinase. The residual expression of the protein is likely due to a slow turnover of EpoR, slow kinetics of Cre-recombination of the floxed EpoR allele, or incomplete infection of the lentivirus. In any case, Cre-dependent reduction of the signal led us to conclude that ctEPOR-AB specifically detects EpoR. Together, these results indicate specific EPOR/EpoR detection with ctEPOR-AB in human and murine cell and tissue extracts.

EPOR protein identification

To test whether the specific band detected in Western blots is indeed EPOR, we performed immunoprecipitations (IP) from UT-7 lysates and subsequent mass spectrometric protein identification. We used covalently immobilized ctEPOR-AB in combination with non-reducing elution conditions to minimize the masking effect of excess antibody heavy chains, which have an apparent electrophoretic mobility similar to the EPOR. After IP with ctEPOR-AB, eluted proteins from ctEPOR-AB protein-G sepharose beads and respective control beads were separated by SDS-PAGE and visualized by colloidal Coomassie staining or immunoblotting. The overlay of the 2 gel images (Fig.2A) was used to identify the region of the Coomassie-stained gel potentially containing the EPOR protein. Identical gel regions from ctEPOR-AB IP and the control IP were excised and subjected to tryptic digestion followed by liquid chromatography coupled to mass spectrometry (LC-MS). Against a common background mainly consisting of chaperone proteins, human EPOR protein was detected in eluates from ctEPOR-AB beads, but not from control beads. The identification of 11 EPOR derived peptides with high mass accuracy at both precursor and fragment ion level resulted in sequence coverage of 22.6% (Fig.2B-C), basically in line with recent LC-MS data on EPOR immunoprecipitates (37). Taken together,

our results show that ctEPOR-AB indeed binds specifically to full-length EPOR. Also, in reducing conditions we could effectively elute EPOR after IP (Fig.2D). Noteworthy, we detected the EPOR protein in Western blots between 59-68 kDa, depending on the gel system and protein molecular weight marker used (see Fig.1, 2A and D and material and methods).

EPOR/EpoR detection by immunocytochemistry

To validate the specificity of ctEPOR-AB on formaldehyde fixed cells, we stained the same antigen with AB directed against different epitopes (38). In EOC-20 cells transduced with an N-terminally HA-tagged human EPOR, anti-HA and ctEPOR-AB double-staining showed almost complete co-localization with most of the signal located intracellularly (Fig.3A). Control EOC-20 cells were negative (Fig.3A). In UT-7 cells, ctEPOR-AB revealed a similar staining pattern (Fig.3B). EPOR staining was co-localized with Golgi staining, indicating detection of a membrane protein (Fig.3C). In addition, ntEPOR-AB and ctEPOR-AB double-stained EPOR in UT-7 cells (Fig.3D). In OCIM-1 cells, ctEPOR-AB also yielded intracellular staining, even though less pronounced compared to UT-7 cells (Fig.3E). Using ctEPOR-AB, we also detected EPOR in human IPS cells (Fig.3F). Moreover, ctEPOR-AB specifically stained HEK293 FT cells transfected with full-length murine *EpoR* (Fig.3G). When tested on cultured primary murine brain cells, ctEPOR-AB stained oligodendrocyte precursor cells (Fig.3H), oligodendrocytes (Fig.3I) and microglia (Fig.3J). These results indicate specific staining of human and mouse EPOR/EpoR by the ctEPOR-AB in cell lines and primary cells.

EpoR detection in the brain of healthy mice

Using ctEPOR-AB on frozen brain sections of healthy young mice, we found EpoR expression mainly in a subpopulation of cells of the oligodendrocyte lineage (Fig.4A). To get better insight at which stages cells of the oligodendrocyte lineage express EpoR, we labelled oligodendrocyte precursor cells by tamoxifen injections in NG2-CreERT2 mice (28). At 72h after the second tamoxifen injection, we identified precursors double-stained for GFP and ctEPOR-AB (GFP+/EPOR+), as well as GFP+/EPOR+ cells with clear morphology (processes with parallel myelin bundles) of already differentiated oligodendrocytes (Fig.4B-B''). Moreover, GFAP+/EPOR+ cells were seen in postnatal neurogenesis areas such as dentate gyrus (Fig.4C) or

subventricular zone (data not shown). These results indicate EPOR expression in differentiating oligodendrocytes and stem cells in the adult neurogenic niches of healthy young mice.

EPOR/EpoR detection in the injured CNS of mice

Next, we stereotactically injected *EPOR*-transduced EOC-20 cells or medium only ('stab wound' analogue) in the motor cortex of adult mice (Fig.4D). This experiment served 2 purposes: [1] to recover defined cells that carry human EPOR in brain sections; [2] to confirm injury-induced endogenous EpoR expression, since in earlier work, we had proposed upregulation of EPOR upon injury (6). At 24h after injection of medium only ('stab wound'), we saw cells with strong ctEPOR-AB signal in close proximity to the injection site (Fig.4E). Many of these cells were GFAP+/EPOR+ (Fig.4F). On the contralateral site, no GFAP+/EPOR+ cells were seen (Fig.4G). In the motor cortex of mice injected with transduced EOC-20 cells (murine microglia cell line), double-labelling with HA-AB and ctEPOR-AB confirmed specific recovery of these cells in frozen sections of paraformaldehyde-perfused mice. Also in this condition, endogenous cells with high EpoR expression were observed in close proximity of the injection site (Fig.4H-H"). These results confirm the pronounced upregulation of EpoR in cells reacting to injury, provoked here by an experimental stab wound.

Upregulation of EPOR in the hippocampal formation of a patient suffering from temporo-mesial complex-focal epilepsy

Formalin-fixed, paraffin-embedded tissue from a patient, who underwent selective unilateral hippocampectomy, was used for immunohistochemical detection of EPOR upregulation under these conditions (Fig.5A). The patient had been suffering from pharmaco-resistant complex-focal seizures of temporo-mesial origin for more than 10 years. Neuropathological analysis of the surgery material revealed hippocampal sclerosis stage Wyler III. EPOR was upregulated in several but not all remaining neurons of CA1 (Fig.5B), of CA4 (Fig.5C) and of the dentate gyrus (Fig.5D), as well as in oligodendrocytes and endothelial cells of capillaries in the adjacent white matter (Fig.5E). Without primary AB, no staining could be detected (Fig.5F). This suggests upregulation of EPOR upon severe chronic distress in different cell types of the human CNS.

DISCUSSION

In the present work, we took the challenge requested for a long time by the scientific community (14, 17-18) to generate a specific AB for valid detection of EPOR in human and murine cells and tissues, with particular focus on the brain. We present here a highly specific polyclonal rabbit AB directed against the intracellular C-terminus of the human EPOR. This AB, referred to as ctEPOR-AB, specifically recognizes EPOR, as proven by mass spectrometry, and has a broad range of documented applications in both human and murine cells and tissues, ranging from Western blotting, flow cytometry, and immunoprecipitation to immunocytochemistry and immunohistochemistry on frozen as well as paraffin-embedded sections. Importantly, by employing this AB, we were able to confirm expression of EPOR in brain cells and its upregulation upon injury (39). Our comprehensive *in vitro* and *in vivo* data clearly reject earlier claims, solely based on *in vitro* studies, that EPOR expression and EPO function outside the hematopoietic system does not exist (15).

The great need for specific EPOR-AB in the field is also reflected by a very recent study of Drorit Neumann and colleagues (37). This group of authors published specific mouse and rat monoclonal EPOR-AB that detect EPOR expression in human cancer cells and tissues (37). Complementary to this approach and with particular focus on the brain, we have developed a highly specific and sensitive polyclonal rabbit AB, ctEPOR-AB, suitable for applications not only in human but also in murine material. Since the polyclonal nature of this AB has limitations, not only due to the restricted life time of a rabbit, we are currently working on further exploitation of the herewith acquired knowledge. Preliminary results of epitope mapping with this polyclonal ctEPOR-AB revealed only few strongly recognized epitopes. These epitopes are presently used for generating specific mouse monoclonal AB. They will be tested alone or in the form of potentially more sensitive 'cocktails', with collective properties similar to the here reported ctEPOR-AB.

With the examples of EPOR expression in the brain shown here, we confirmed earlier work of ourselves and others which needed in the past additional methods for validation, and still left doubts in the scientific community due to the non-specificity of

previous EPOR-AB. For instance, GFAP positive stem cells in the adult neurogenic niches showed EpoR immunoreactivity here, which is in line with reports demonstrating distinct effects of EPO on adult neural stem cells (40-41). Also, studies identifying EPO as inducer of oligodendrocyte precursor cell differentiation (42-43) are now further supported by the detection of specific EPOR binding sites in culture and brain sections. Importantly, the role of the EPO/EPOR system in response to brain injury (5-6) is confirmed with our stab wound approach.

To conclude, based on the here reported novel tool, it will now be possible to investigate the role of EPOR in the intact and injured human and murine brain in more detail. This, in turn, will facilitate the development of EPO for therapeutic use outside the hematopoietic system.

UNCORRECTED PROOF

ACKNOWLEDGEMENTS

This work was supported by ZIM-BWMI, the Max Planck Society, the Deutsche Forschungsgemeinschaft (Center for Nanoscale Microscopy & Molecular Physiology of the Brain, SFB-TRR43), EXTRABRAIN EU-FP7, and the Niedersachsen-Research Network on Neuroinfectiology (N-RENNT).

CONFLICTS OF INTEREST

Herbert Stadler is member of the board of and holds stocks in Synaptic Systems GmbH. Henrik Martens, Christian Erck and Tekla Kolbow are full-time employees of Synaptic Systems GmbH. All other authors declare no conflict of interest.

AUTHOR CONTRIBUTIONS

CO, HM, and HE planned, supervised, and coordinated the project. HM, with the assistance of CE and TK, designed immunization strategies and performed antiserum purification and first antibody characterization work. CO carried out Western blotting, immunoprecipitation, cell culture work, and mouse experiments including fluorescent immunostainings and confocal images, supported in relevant parts by IH, BO, UKP, SG, and BA. OJ, with the help of DH conducted the mass spectrometry work. WSS was responsible for human brain immunohistochemistry. KAN, HS, HK, MPZ, WHZ, and WSS were instrumental for aspects of study design related to their respective expertise and data interpretation. CO and HE wrote the paper. All authors read and approved the final version of the manuscript.

FIGURE LEGENDS

Figure 1: Functional EPOR validation and EPOR/EpoR detection using ctEPOR-AB in Western blots. (A) Incubation of EPO-dependent UT-7 cells (after 12h of EPO deprivation) for 15min with increasing EPO concentrations induced STAT5 phosphorylation. **(B)** Incubation of OCIM-1 cells for 15min with increasing EPO concentrations induced STAT5 phosphorylation. **(C)** Cell counts of EPO-dependent UT-7 cultures 72h after seeding in presence and absence of EPO (n=6, mean±SEM; p<0.0001). **(D)** Cell death in EPO-dependent UT-7 cultures 72h after seeding in presence and absence of EPO (n=5, mean±SEM; p<0.03). **(E)** Incubation of EOC-20 cells transduced with HA-tagged human EPOR for 10min with increasing EPO concentrations induced MAPK phosphorylation. **(F)** EPOR Western blot using ctEPOR-AB on transfected HEK293 FT cell lysates (truncated HA-EPOR: human EPOR lacking the C-terminus, HA-tag at the N-terminus; control vector: anchored human EPOR without N-terminus and C-terminus). **(G)** HA Western blot of the same transfected HEK293 FT cell lysates used in (F). **(H)** EPOR Western blot using ctEPOR-AB on EOC-20 cell lysates transduced with N-terminally HA-tagged human EPOR and respective controls. **(I)** HA Western blot of the same EOC-20 cell lysates used in (H). **(J)** EPOR Western blot using ctEPOR-AB on UT-7 and OCIM-1 cell lysates. **(K)** Flow cytometry of fixed UT-7 cells stained with ctEPOR-AB and Alexa488 donkey anti-rabbit secondary AB; as control secondary AB only. **(L)** EPOR detection in human placenta and human fetal brain using ctEPOR-AB. **(M)** Detection of murine EpoR in transfected HEK293 FT cells overexpressing murine *EpoR*, mouse fetal liver and mouse primary oligodendrocytes using ctEPOR-AB. **(N)** Lentivirus-mediated conditional *EpoR* knockout in primary *EpoR-fl/fl* mouse astrocytes; anti-alpha tubulin as stably expressed comparator.

Figure 2: EPOR immunoprecipitation using ctEPOR-AB and protein identification by mass spectrometry. (A) Colloidal Coomassie staining and immunoblot of the same EPOR immunoprecipitation using ctEPOR-AB from UT-7 protein lysates. The overlay was used to determine the region to be excised from the Coomassie gel for subsequent mass spectrometric protein identification (area indicated by rectangles; abbreviations: FT=flow through, IP=immunoprecipitation).

(B) Amino acid sequence of EPOR (UniProtKB/Swiss-Prot P19235). Peptides identified by mass spectrometry are indicated in red. Note that large parts of the EPOR precursor sequence (indicated in italics) cannot be covered in a standard proteomic experiment with tryptic cleavage as they are either modified (amino acids 1-34, signal peptide; 57-89, N-glycosylation site), attached to the transmembrane domain (224-275) or too large (> 5kDa) to reveal useful information by mass spectrometric sequencing (379-453, 454-508). **(C)** Table with details on peptide identification. Columns show from left to right: numbering of tryptic peptides; numbering of amino acids according to the sequence in **B**; peptide sequence (c, carboxamidomethyl-Cys); observed and calculated mass of the singly protonated peptide; peptide mass deviation in ppm; PLGS score; number of b-y fragment ions; root mean square fragment mass deviation in ppm. **(D)** Immunoblot of EPOR immunoprecipitation using ctEPOR-AB from UT-7 lysates. In contrast to the immunoprecipitation used for mass spectrometry, EPOR was eluted from the beads in reducing conditions (Laemmli buffer with β -mercaptoethanol, abbreviations: FT=flow through, IP=immunoprecipitation, Ig HC=immunoglobulin heavy chains, Ig LC=immunoglobulin light chains). The prominent band at around 40kDa in both IP conditions has to be an immunoglobulin fragment eluted from the beads in the reducing condition only, since it was not eluted without β -mercaptoethanol (see subpanel 2A immunoblot).

Figure 3: Detection of EPOR by immunocytochemistry: **(A)** EPOR detection using ctEPOR-AB and monoclonal HA-AB on transduced (N-terminally HA-tagged human EPOR, upper row) and control (lower row) EOC-20 cells. **(B)** EPOR staining with ctEPOR-AB on EPO-dependent UT-7 cells. **(C)** Double-Immunostaining of UT-7 cells with anti-GM130 AB as marker for the Golgi apparatus and ctEPOR-AB. **(D)** EPOR double staining of UT-7 cells with ntEPOR AB and ctEPOR-AB. **(E)** EPOR staining with ctEPOR-AB on OCIM-1 cells. **(F)** Distinct EPOR staining in human Oct-4+ IPS cells using ctEPOR-AB. **(G)** EpoR staining with ctEPOR-AB of HEK 293 FT cells transfected with full-length murine *EpoR*. Neighbouring non-transfected cells show no immunofluorescence. **(H)** EpoR and NG2 double-staining with ctEPOR-AB in primary mouse oligodendrocyte precursor cells. **(I)** EpoR and CC-1 double-staining

of primary mouse oligodendrocytes with ctEPOR-AB. **(J)** Detection of EpoR in primary mouse microglia using ctEPOR-AB and lectin as counterstain.

Figure 4: EPOR detection using ctEPOR-AB in healthy and injured mouse brain by immunohistochemistry: **(A)** EpoR staining in a subpopulation of CC-1 positive mature oligodendrocytes in the neocortex of a 5 week-old healthy mouse. **(B, B', B'')** EpoR staining in the hippocampus of a 5 week-old NG2-CreERT2:R26-td-tomato-mEGFP mouse. Some oligodendrocyte precursor cells (arrow head) and newly differentiated oligodendrocytes (arrow) express EpoR. Both cell types are endogenously labelled with membrane-tagged EGFP. **(C)** EpoR staining of GFAP+ cellular processes in the dentate gyrus of a 5 week-old mouse (arrow heads). **(D)** Overview of the injection site in the motor cortex of an 8 week-old mouse injected with medium only ('stab wound' analogue). The section was stained for neuronal nuclei with NeuN and for EpoR with ctEPOR-AB. **(E)** Close-up of the white-rectangle region in (D) shows reactive cells with up-regulated EpoR expression. **(F)** Many of the cells at the injection site with up-regulated EpoR expression are GFAP+ (arrow heads). **(G)** Contralateral to the injection site, GFAP+ cells show no EpoR expression at 24h after lesion. **(H, H', H'')** Shown is EPOR and HA double-labelling of injected EOC-20 microglial cells transduced with an HA-tagged human *EPOR*. In addition, HA-negative cells at the injection site show strong EpoR expression (arrow heads).

Figure 5: EPOR upregulation in neurons and oligodendrocytes of the hippocampal formation of a patient suffering from temporo-mesial complex-focal epilepsy as demonstrated by immunohistochemistry using ctEPOR-AB. **(A)** Overview of the surgical sample stained with ctEPOR-AB. **(B)** Upregulation of EPOR, visualized by brown colour of the AEC-chromogen, in some (arrows) but not all (arrow heads) neurons of the CA1 region. **(C)** EPOR positive neurons in the CA4 region (arrows). **(D)** Dentate gyrus neurons (arrows) expressing EPOR. **(E)** EPOR positive oligodendrocytes (arrows) as well as endothelial cells of capillaries (arrow heads) in the adjacent white matter. **(F)** No staining was observed when omitting the primary antibody.

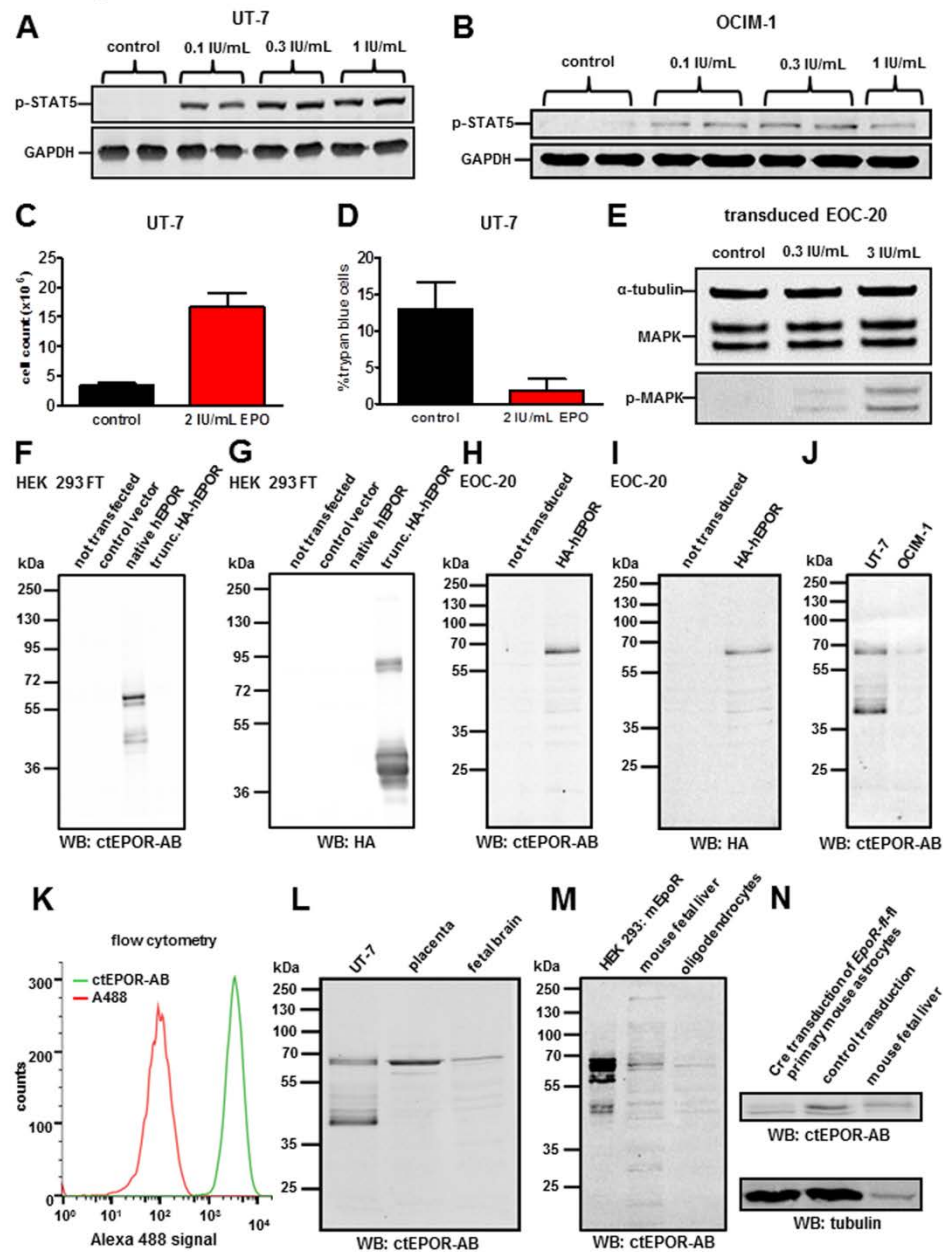
REFERENCES

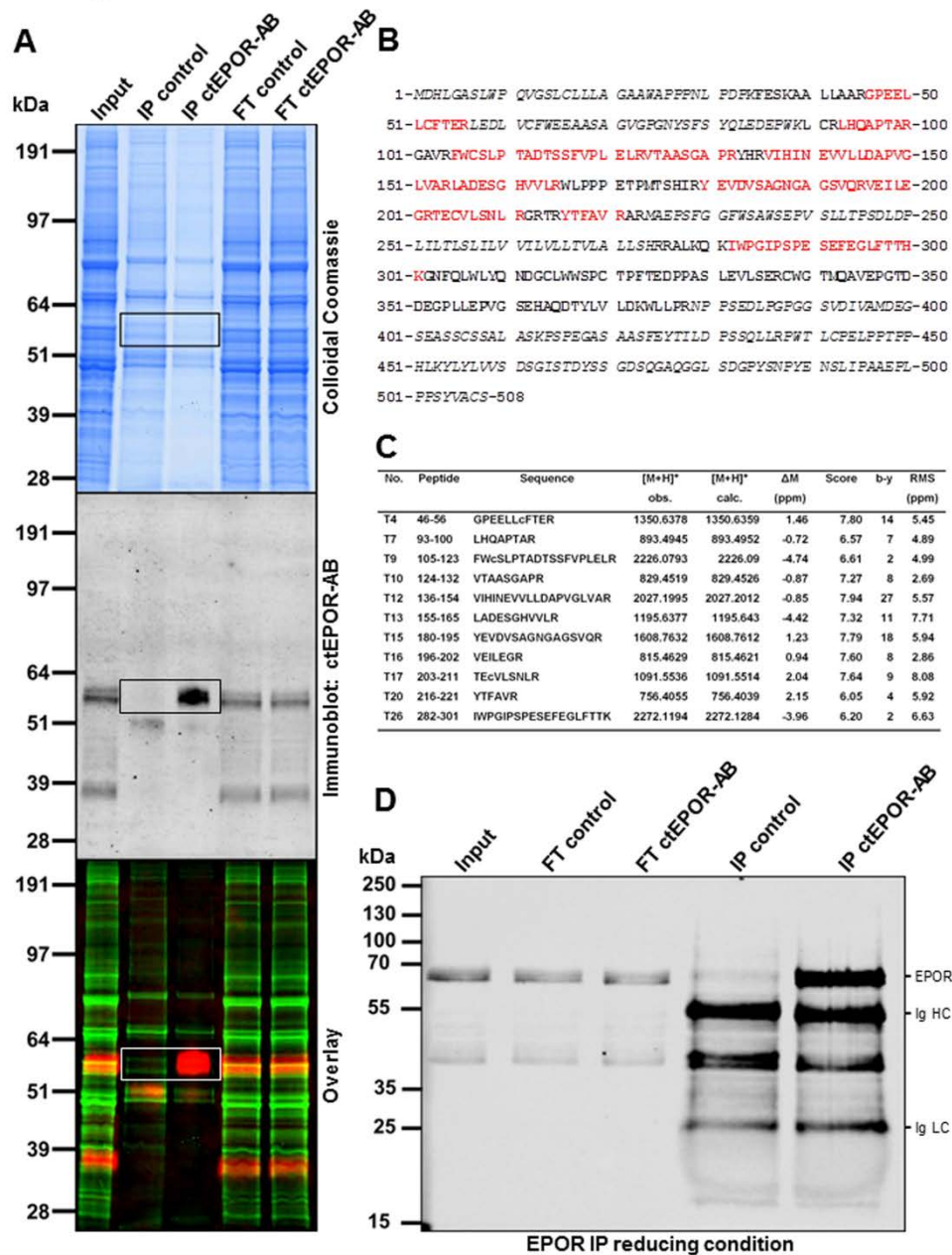
1. Brines M, Cerami A. (2005) Emerging biological roles for erythropoietin in the nervous system. *Nat Rev Neurosci* **6**: 484-494.
2. Jelkmann W. (2007) Erythropoietin after a century of research: younger than ever. *Eur J Haematol* **78**: 183-205.
3. Jelkmann W. (2013) Physiology and pharmacology of erythropoietin. *Transfus Med Hemother* **40**: 302-309.
4. Arcasoy MO. (2008) The non-haematopoietic biological effects of erythropoietin. *Br J Haematol* **141**: 14-31.
5. Sargin D, Friedrichs H, El-Kordi A, Ehrenreich H. (2010) Erythropoietin as neuroprotective and neuroregenerative treatment strategy: comprehensive overview of 12 years of preclinical and clinical research. *Best Pract Res Clin Anaesthesiol* **24**: 573-594.
6. Siren AL, Fasshauer T, Bartels C, Ehrenreich H. (2009) Therapeutic potential of erythropoietin and its structural or functional variants in the nervous system. *Neurotherapeutics* **6**: 108-127.
7. Miskowiak KW, Vinberg M, Harmer CJ, Ehrenreich H, Kessing LV. (2012) Erythropoietin: a candidate treatment for mood symptoms and memory dysfunction in depression. *Psychopharmacology (Berl)* **219**: 687-698.
8. D'Andrea AD, Lodish HF, Wong GG. (1989) Expression cloning of the murine erythropoietin receptor. *Cell* **57**: 277-285.
9. Jones SS, D'Andrea AD, Haines LL, Wong GG. (1990) Human erythropoietin receptor: cloning, expression, and biologic characterization. *Blood* **76**: 31-35.
10. Noguchi CT, *et al.* (1991) Cloning of the human erythropoietin receptor gene. *Blood* **78**: 2548-2556.
11. Elliott S, *et al.* (2010) Identification of a sensitive anti-erythropoietin receptor monoclonal antibody allows detection of low levels of EpoR in cells. *J Immunol Methods* **352**: 126-139.
12. Noguchi CT, Wang L, Rogers HM, Teng R, Jia Y. (2008) Survival and proliferative roles of erythropoietin beyond the erythroid lineage. *Expert Rev Mol Med* **10**: e36.
13. Siren AL, *et al.* (2001) Erythropoietin prevents neuronal apoptosis after cerebral ischemia and metabolic stress. *Proc Natl Acad Sci U S A* **98**: 4044-4049.
14. Elliott S, *et al.* (2006) Anti-Epo receptor antibodies do not predict Epo receptor expression. *Blood* **107**: 1892-1895.
15. Sinclair AM, *et al.* (2010) Functional erythropoietin receptor is undetectable in endothelial, cardiac, neuronal, and renal cells. *Blood* **115**: 4264-4272.
16. Ghezzi P, *et al.* (2010) Erythropoietin: not just about erythropoiesis. *Lancet* **375**: 2142.
17. Kirkeby A, van Beek J, Nielsen J, Leist M, Helboe L. (2007) Functional and immunochemical characterisation of different antibodies against the erythropoietin receptor. *J Neurosci Methods* **164**: 50-58.
18. Brown WM, *et al.* (2007) Erythropoietin receptor expression in non-small cell lung carcinoma: a question of antibody specificity. *Stem Cells* **25**: 718-722.
19. Yu X, *et al.* (2002) Erythropoietin receptor signalling is required for normal brain development. *Development* **129**: 505-516.

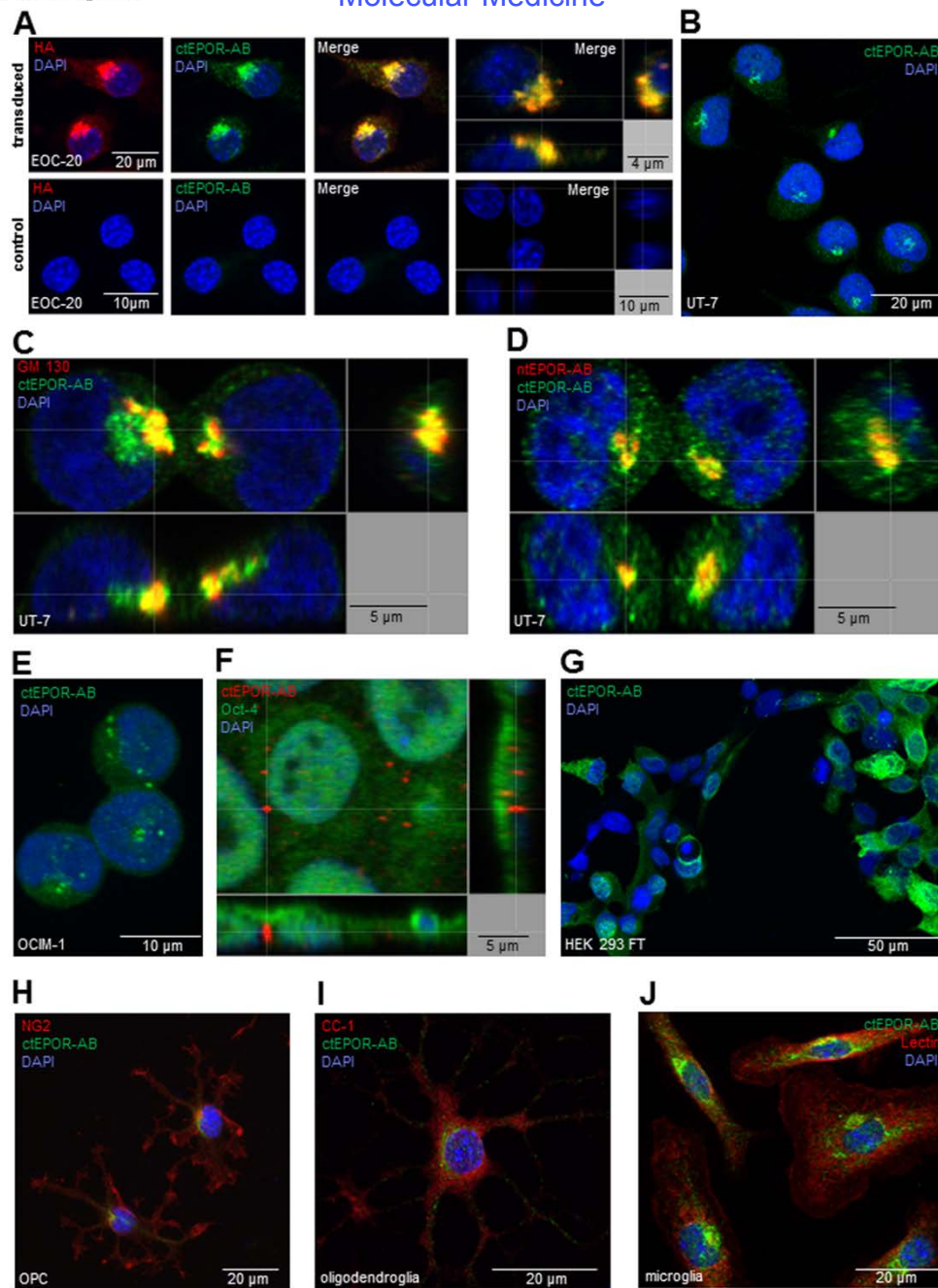
20. Tsai PT, *et al.* (2006) A critical role of erythropoietin receptor in neurogenesis and post-stroke recovery. *J Neurosci* **26**: 1269-1274.
21. Ehrenreich H, *et al.* (2005) A hematopoietic growth factor, thrombopoietin, has a proapoptotic role in the brain. *Proc Natl Acad Sci U S A* **102**: 862-867.
22. Digicaylioglu M, *et al.* (1995) Localization of specific erythropoietin binding sites in defined areas of the mouse brain. *Proc Natl Acad Sci U S A* **92**: 3717-3720.
23. Ehrenreich H, *et al.* (2004) Erythropoietin: a candidate compound for neuroprotection in schizophrenia. *Mol Psychiatry* **9**: 42-54.
24. Mitkovski M, *et al.* (2015) Erythropoietin dampens injury-induced microglial motility. *J Cereb Blood Flow Metab* **35**: 1233-1236.
25. Aggarwal S, *et al.* (2013) Myelin membrane assembly is driven by a phase transition of myelin basic proteins into a cohesive protein meshwork. *PLoS Biol* **11**: e1001577.
26. Pyott SJ, Rosenmund C. (2002) The effects of temperature on vesicular supply and release in autaptic cultures of rat and mouse hippocampal neurons. *J Physiol* **539**: 523-535.
27. Becker V, *et al.* (2010) Covering a broad dynamic range: information processing at the erythropoietin receptor. *Science* **328**: 1404-1408.
28. Huang W, *et al.* (2014) Novel NG2-CreERT2 knock-in mice demonstrate heterogeneous differentiation potential of NG2 glia during development. *Glia* **62**: 896-913.
29. Muzumdar MD, Tasic B, Miyamichi K, Li L, Luo L. (2007) A global double-fluorescent Cre reporter mouse. *Genesis* **45**: 593-605.
30. Wessel D, Flugge UI. (1984) A method for the quantitative recovery of protein in dilute solution in the presence of detergents and lipids. *Anal Biochem* **138**: 141-143.
31. Schmidt C, Hesse D, Raabe M, Urlaub H, Jahn O. (2013) An automated in-gel digestion/iTRAQ-labeling workflow for robust quantification of gel-separated proteins. *Proteomics* **13**: 1417-1422.
32. Silva JC, Gorenstein MV, Li GZ, Vissers JP, Geromanos SJ. (2006) Absolute quantification of proteins by LCMSE: a virtue of parallel MS acquisition. *Mol Cell Proteomics* **5**: 144-156.
33. Silva JC, *et al.* (2005) Quantitative proteomic analysis by accurate mass retention time pairs. *Anal Chem* **77**: 2187-2200.
34. Geromanos SJ, Hughes C, Ciavarini S, Vissers JP, Langridge JI. (2012) Using ion purity scores for enhancing quantitative accuracy and precision in complex proteomics samples. *Anal Bioanal Chem* **404**: 1127-1139.
35. Distler U, *et al.* (2014) Drift time-specific collision energies enable deep-coverage data-independent acquisition proteomics. *Nat Methods* **11**: 167-170.
36. Li GZ, *et al.* (2009) Database searching and accounting of multiplexed precursor and product ion spectra from the data independent analysis of simple and complex peptide mixtures. *Proteomics* **9**: 1696-1719.
37. Maxwell P, *et al.* (2015) Novel antibodies directed against the human erythropoietin receptor: creating a basis for clinical implementation. *Br J Haematol* **168**: 429-442.
38. Saper CB. (2005) An open letter to our readers on the use of antibodies. *J Comp Neurol* **493**: 477-478.

39. Siren AL, *et al.* (2001) Erythropoietin and erythropoietin receptor in human ischemic/hypoxic brain. *Acta Neuropathol* **101**: 271-276.
40. Shingo T, Sorokan ST, Shimazaki T, Weiss S. (2001) Erythropoietin regulates the in vitro and in vivo production of neuronal progenitors by mammalian forebrain neural stem cells. *J Neurosci* **21**: 9733-9743.
41. Ransome MJ, Turnley AM. (2007) Systemically delivered Erythropoietin transiently enhances adult hippocampal neurogenesis. *J Neurochem* **102**: 1953-1965.
42. Jantzie LL, Miller RH, Robinson S. (2013) Erythropoietin signaling promotes oligodendrocyte development following prenatal systemic hypoxic-ischemic brain injury. *Pediatr Res* **74**: 658-667.
43. Kako E, *et al.* (2012) Subventricular zone-derived oligodendrogenesis in injured neonatal white matter in mice enhanced by a nonerythropoietic erythropoietin derivative. *Stem Cells* **30**: 2234-2247.

Ott et al Figure 1







Ott et al Figure 4

